Oceanologia (2018) 60, 264—276

Available online at www.sciencedirect.com

ScienceDirect

journal homepage: www.journals.elsevier.com/oceanologia/

ORIGINAL RESEARCH ARTICLE

Coastal hydrodynamics beyond the surf zone of the south Baltic Sea

Rafał Ostrowski [a,*], **Magdalena Stella** [a], **Piotr Szmytkiewicz** [a], **Jarosław Kapiński** [b], **Tomasz Marcinkowski** [b]

[a] *Institute of Hydro-Engineering, Polish Academy of Sciences, Gdańsk, Poland*
[b] *Maritime Institute, Gdańsk, Poland*

Received 4 May 2017; accepted 30 November 2017
Available online 16 December 2017

KEYWORDS
Wind-driven current;
Wave-induced nearbed oscillations;
Bed shear stresses;
Friction velocity;
Baltic Sea;
Moderate depths

Summary The paper presents experimental and theoretical investigations of hydrodynamic processes in a coastal region located close to the seaward boundary of the surf zone. The analysis is based on field data collected near Lubiatowo (Poland) by measuring equipment operated simultaneously by the Institute of Hydro-Engineering of the Polish Academy of Sciences (IBW PAN) and the Maritime Institute in Gdańsk (IMG). The data consist of wind velocity and direction measured at the IBW PAN Coastal Research Station (CRS) in Lubiatowo, deep-water wave buoy records, current profiles and sea bottom sediment parameters. Mean flow velocities measured in the entire water column have almost the same direction as wind. Nearbed flow velocities induced by waves and currents, as well as bed shear stresses, are modelled theoretically to determine sediment motion regimes in the area. It appears that the nonlinear wave—current interaction generates bed shear stresses greater than those that would result from the superposition of the impacts of waves and currents separately. The paper discusses the possibility of occasional intensive sediment transport and the occurrence of distinct seabed changes at greater coastal water depths adjacent to the surf zone. It was found that this can happen under the joint influence of waves and wind-driven currents.

* Corresponding author at: IBW PAN, 7 Kościerska, 80-328 Gdańsk, Poland. Tel. +48 58 522 29 00. Fax. +48 58 552 42 11.
E-mail address: rafal.o@ibwpan.gda.pl (R. Ostrowski).
Peer review under the responsibility of Institute of Oceanology of the Polish Academy of Sciences.

ELSEVIER Production and hosting by Elsevier

https://doi.org/10.1016/j.oceano.2017.11.007

1. Introduction

At large water depths, the influence of wave-induced oscillatory flows and wave-driven currents on the sandy seabed is much less intensive than in the nearshore region. Sediment motion rates in the offshore areas are significantly smaller, and therefore seabed changes become less noticeable. At such locations, the motion of water (and consequently sediment movement) in the nearbed layer can be related to currents typically occurring in the open sea, for instance, drift currents. In tidal seas, such as the North Sea, the occurrence and movement of large sandy bed forms called sand waves or sand banks at depths of 20—30 m are closely associated with tidal phenomena, see Carbajal and Montaño (2001) and Hulscher and van den Brink (2001). However, Belibassakis and Karathanasi (2017) have recently shown that in a tidal basin (Saronic-Athens Gulf) a complex configuration of the coastline orientation, bathymetry, wave conditions and strong winds during extreme storms makes tidal currents less important to sediment transport. Similar large bed forms have also been observed, albeit sporadically, in a non-tidal environment, namely in the south Baltic coastal areas at depths of 15—30 m, see Rudowski et al. (2008). Moreover, it was observed that, in the south-eastern part of the Baltic Sea in the vicinity of Władysławowo (with water depths between 14 and 17.3 m), post-dredging pits, 11 months after sand extraction, were shallower by about 2—2.5 m, and traces left by a trailing suction hopper dredger disappeared completely. It is believed that the cause of this phenomenon was both slope slipping and the supply of deposits from the surrounding area. Another study in the southern Baltic Sea indicates that at depths of 15—20 m, a 0.4—0.8 m thick sand layer moves under storm conditions (Uścinowicz et al., 2014).

Open sea currents, such as gradient, geostrophic, inertial and gravitational currents or those arising as a result of seiches, are unlikely to generate intensive sediment transport at depths of less than 30 m. Recent research by Ostrowski and Stella (2016) shows that, aside from waves, wind-driven currents have the most important impact on hydrodynamic processes at a depth of ca. 20 m.

In the coastal zone (particularly in the surf zone), wind-driven flows are dominated by wave-driven currents. The role of wind-driven currents in marine hydrodynamics increases in regions more distant from the shoreline. On the other hand, the influence of wind-induced currents on bottom sediments decreases at bigger depths. Precise determination of the boundary between the zones of domination of wave-driven currents and wind-driven currents is difficult. This is mainly due to the fact that the parameters of both types of currents strongly depend on instantaneous local conditions: wind speed and direction, wave characteristics (height, period and direction of propagation) and the morphology of the coastal bottom. On the basis of field data collected at CRS Lubiatowo and theoretical modelling with the commercial software MIKE 21, Sokolov and Chubarenko (2012) found the wind-induced component of currents in the surf zone to be quite high. It appears that wind can contribute almost 50% to the generation of the longshore current if it blows parallel to the shoreline and more than 20% if it blows at an angle of 45% to the shoreline. In all cases, however, the wave-driven longshore current is the predominant flow in the surf zone. The situation seawards of the surf zone is most probably different.

In coastal areas of the Baltic Sea, the influence of the Coriolis effect may be neglected. A wind-driven current occurring in shallow basins has almost the same direction in the water column as the wind blowing over the water surface. Because the surface Ekman layer and the bottom Ekman layer overlap, the development of the Ekman spiral is hindered, and the wind-induced flow takes place in the wind direction (Krauss, 2001; Trzeciak, 2000; Valle-Levinson, 2016). The present paper deals with wind-driven currents occurring locally and temporarily. Hence, the wind-driven current velocity profile can be described by a directionally invariable distribution.

Wave-induced orbital nearbed velocities also have some impact on the sea bottom beyond the surf zone. The seaward boundary of this influence is conventionally related to the so-called depth of closure (h_c), at which even stormy waves do not cause intensive sediment transport (the so-called sheet flow). The corresponding extreme wave conditions are most often represented by the "effective" significant wave height (H_e), which is exceeded only 12 h per year, or 0.137% of the time. Simple formulas derived by Birkemeier (1985), or earlier by Hallermeier (1978, 1981), for the assessment of the depth of closure h_c from the effective significant wave height (H_e) and period (T_e), are discussed, for example, by Dean (2002). On a second front, the depth of closure h_c can be determined directly from bathymetric changes if only sufficient data are available.

For the multi-bar shore, characteristic of the south Baltic Sea, Cerkowniak et al. (2015a) obtained (from bathymetric surveys) actual values of the depth of closure h_c = 6.0—7.7 m, greater than the ones calculated using parameters of the effective significant wave height (h_c = 4.9—6.5 m). According to Cerkowniak et al. (2015b), wave-induced bed shear stresses during storms (with the deep water significant wave height H_s exceeding 3.5 m) cause intensive sediment transport (sheet flow) even at depths of 13—15 m. Such wave conditions, however, last no longer than 24 h per year, and it is interesting whether, by themselves, they cause distinct changes in the sea bottom, leading to the appearance and movement of large offshore bed forms. The research finding by Cerkowniak et al. (2015a) that direct bathymetric measurements of the shore yield larger values of the depth of closure than do theoretical calculations based on waves only, leads to the conclusion that another factor should be included. One should take into account that such forms at these depths can probably appear and evolve only if stormy waves are accompanied by strong sea currents.

The above considerations give rise to a hypothesis about an important role of currents typically occurring beyond the surf zone and interacting with wave-induced oscillatory flows. Under storm conditions, this interaction presumably generates bed shear stresses sufficient to cause intensive sediment transport and, consequently, distinct sea bottom evolution.

Verification of the above hypothesis requires a precise determination of the sediment driving forces (represented here by bed shear stresses) resulting from the interaction of nearbed wave-induced oscillations (orbital velocities) with steady currents occurring during severe storms at the seaward boundary of the surf zone and beyond the surf zone.

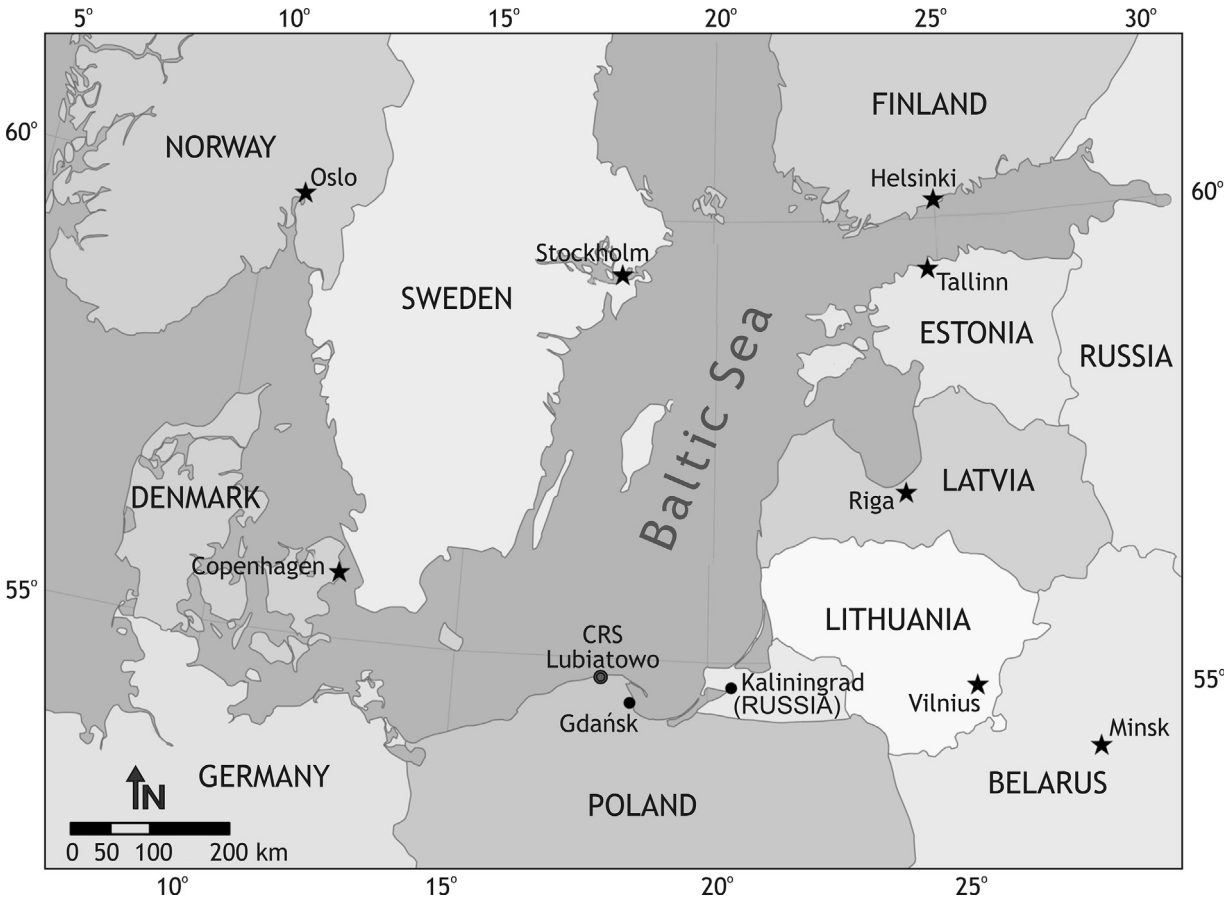

Figure 1 Location of CRS Lubiatowo on the Baltic coast.

The present study tackles this issue by analysing field data collected near Lubiatowo, Poland, as well as by mathematical modelling. Together with analysis of wave-current and wind data, an accurate theoretical description of the Shields parameter θ in the case of a synergic action of waves and the wind-driven current is the main purpose of this study.

2. Study site

The present study is based on the wind, wave and current data collected in the period from April 26, 2014 to June 30, 2014, as well as some other archival information and data, mainly concerning sediments.

The measurements were carried out by the Institute of Hydro-Engineering of the Polish Academy of Sciences (IBW PAN) and the Maritime Institute in Gdańsk (IMG) using scientific instruments located at the IBW PAN Coastal Research Station (CRS) in Lubiatowo and its vicinity. The study area of CRS Lubiatowo is situated about 70 km NW of Gdańsk (see Fig. 1). The hydrodynamics, lithodynamics and morphodynamics in the region of Lubiatowo are typical of the south Baltic sandy coast (see Cerkowniak et al., 2017; Ostrowski et al., 2015). For purposes of the present study, offshore wave buoy data and current profiles were used, as well as wind data collected on land at CRS Lubiatowo. In addition, results of sediment sampling and grain size analysis were taken into account.

The sea shore near Lubiatowo is mildly sloped (with an inclination of 1—2%) and consists of quartz sand having the median grain diameter d_{50} in the range from 0.1 to 0.4 mm (mostly 0.15—0.25 mm). The sediment density amounts to ρ_s = 2650 kg m^{-3}. Cross-shore bathymetric profiles display 3—4 stable bars and an additional, ephemeral one occurring close to the shoreline. Such a multi-bar profile of the sea bottom is favourable to gradual wave energy dissipation, taking place by multiple wave breaking, see Pruszak et al. (2008).

3. Methods of field measurements

The offshore measurements near CRS Lubiatowo were carried out by means of an acoustic current profiler with an attached surface wave measurement module AWAC produced by Nortek and operating at 600 kHz transmission frequency. The device was installed with transducers facing up on a bottom-resting frame at a distance of about 1.47 Nm (i.e. 2.72 km) from the shoreline, where the mean water depth amounted to 17 m, at coordinates 54°50.48′N and 17°53.09′E. Wave data were measured continuously once an hour for about 17 min (2048 samples recorded with a frequency of 2 Hz) and then averaged. Water flows were measured in 1 m thick layers once an hour, and they were averaged for 2-min recordings registered with 1 Hz frequency. The nearbed layer (about 1 m thick) was excluded from flow measurements for

Figure 2 Anemometer on top of a mast at CRS Lubiatowo.

technical reasons (the height of the frame on which the instrument was mounted and the so-called blanking distance, i.e. direct water body thickness to transducers, where the accuracy of measurements was not acceptable). Additionally, the results of flow measurements in the surface water layer (from 5 to 10% of the total depth) have limited reliability due to side-lobe interference. Therefore, this layer should be analysed with some care. Raw and processed wave data were collected in the internal memory of the instrument and delivered for analysis during maintenance cruises.

The wind data were collected by a cup anemometer SW-48 (produced by MORS, Poland) installed on a 22 m mast. The mast is located on land close to CRS Lubiatowo (54°48.70′N, 17°50.43′E), at a distance of about 150 m from the shoreline. The anemometer is installed a few metres above the upper branches of nearby trees (Fig. 2).

4. Wind records correction

The location of the anemometer does not satisfy standards of meteorological monitoring, and the measurements of wind parameters (particularly velocity) are biased. Although the mast is 12 m higher than indicated in the standards (10 m), the increased terrain roughness, resulting from the presence of trees, makes that the recorded wind speed smaller than it would be over a flat ground, without trees or other obstacles, as required at state meteorological stations in Poland. It was necessary to investigate the differences between the wind speed measured at CRS Lubiatowo and the expected wind speed near the study site. Due to the lack of direct wind records from the time and place of the current measurements, it was necessary to obtain them in a different way. To do so, the authors compared measured data with values obtained from the ICM operating model (UM model) provided by SatBaltyk System (http://satbaltyk.iopan.gda.pl). These data were deemed reliable due to constant data assimilation and the calibration of the model with data measured at various meteorological stations. In addition, a visual analysis and comparison of ICM data with Lubiatowo measurements showed that wind directions were almost the same in both data series. Hourly time series of wind velocities were analysed for the coordinates 54°50′N, 17°50′E for the time period from May 08, 2016 to February 06, 2017, the only period for which data were available on the SatBaltyk System.

A rough analysis of wind data collected at CRS Lubiatowo and determined over the sea from ICM data shows that wind velocities measured in Lubiatowo are significantly lower than those obtained from ICM (Fig. 4). The maximum wind velocities recorded at CRS Lubiatowo slightly exceeded 10 m s^{-1} on only two occasions, whereas ICM Model wind speeds exceeded 15 m s^{-1} several times, reaching up to 20 m s^{-1} under extreme conditions.

The present study includes, among others, investigations of wind-induced water flow at the location of the current profiler, beyond the surf zone, at a depth of 17 m. As mentioned above, wind measurements from CRS Lubiatowo are biased and should therefore be recalculated to become representative of the location considered. To this end, a joint analysis of wind parameters collected at CRS Lubiatowo and determined over the sea by the UM model (provided by the SatBaltyk System) was carried out. Statistical analysis of these two data series shows strong, positive correlation, with the correlation coefficient r of 0.78 (Fig. 3).

It was found that to obtain a reliable wind speed at the current monitoring point, wind velocities measured in Lubiatowo ought to be recalculated by the following regression equation:

$$y = 1.92 + 1.76x. \quad (1)$$

5. Measured results

Time series of selected parameters are shown in Figs. 4 and 6—8. The results of the wind speed recalculation are shown in Fig. 5, and the significant wave height record is plotted in Fig. 6. It can be seen in Fig. 6 that, for the period considered, the significant wave height amounts to 2—2.5 m during storms, and up to 2.76 m under extreme conditions. Figs. 7 and 8 suggest, as could be expected, that the currents near the surface are stronger than the nearbed currents, reaching maximum velocities of about 0.6 m s^{-1} and 0.4 m s^{-1}, respectively.

Although the plots of wind speed and wave height look different, the extreme data occur at the same time. The wind

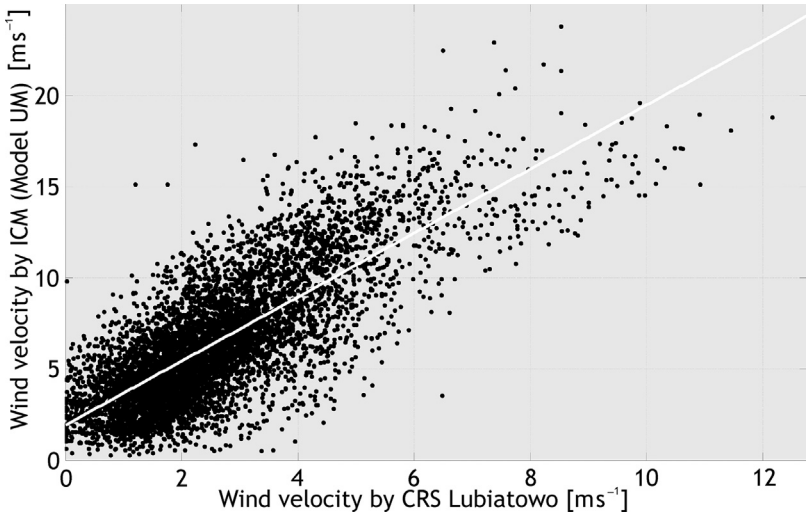

Figure 3 Scatterplot of wind measured at CRS Lubiatowo against ICM wind velocities for the period from May 08, 2016 to February 06, 2017.

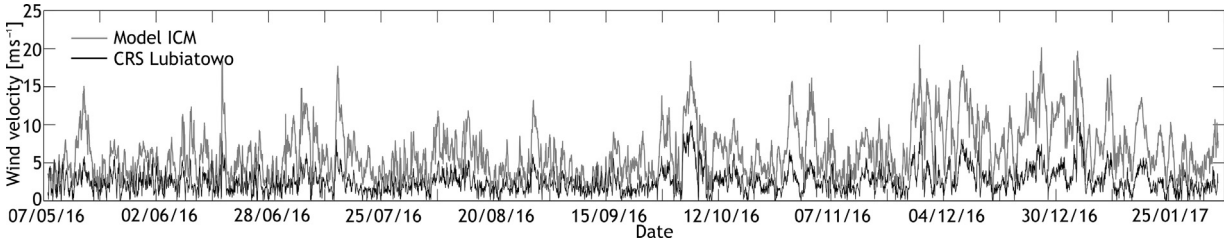

Figure 4 Time series of the mean hourly wind speed obtained from ICM (grey line) (data provided by SatBaltyk System) and measured at CRS Lubiatowo (black line) (both data sets from May 08, 2016 to February 06, 2017).

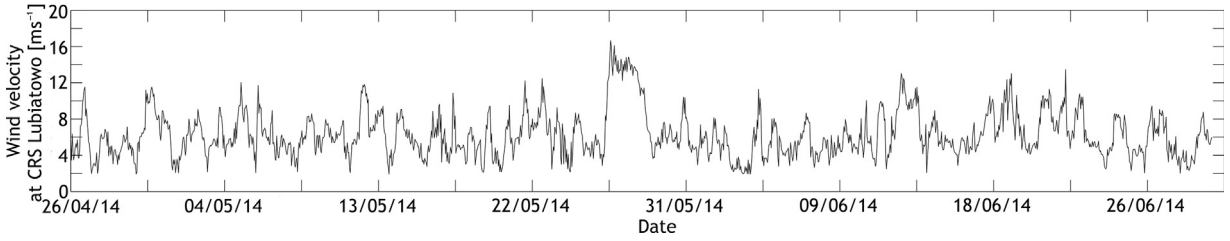

Figure 5 Wind speed measurements at CRS Lubiatowo recalculated by a regression equation for the time period from April 26, 2014 to June 30, 2014.

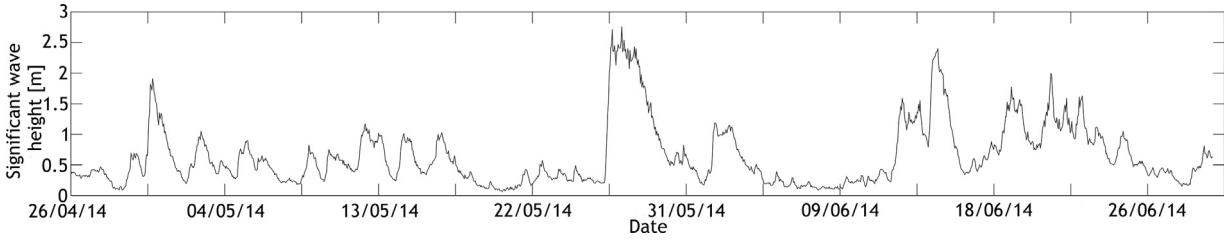

Figure 6 Hourly time series of the significant wave height in the vicinity of CRS Lubiatowo for the time period from April 26, 2014 to June 30, 2014.

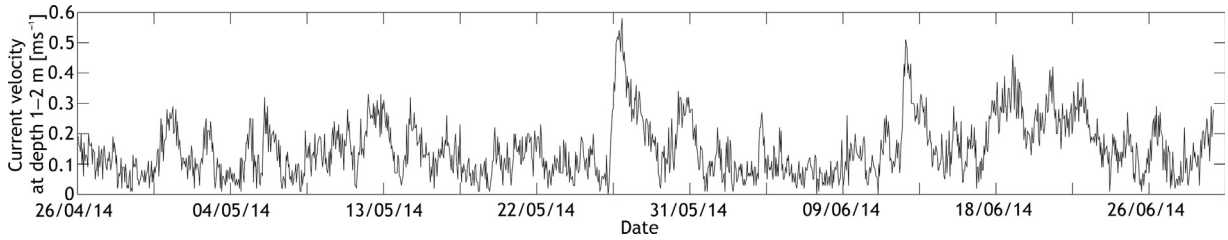

Figure 7 Time series of the mean hourly flow velocity in the subsurface layer (15–16 m above the bottom) for the time period from April 26, 2014 to June 30, 2014.

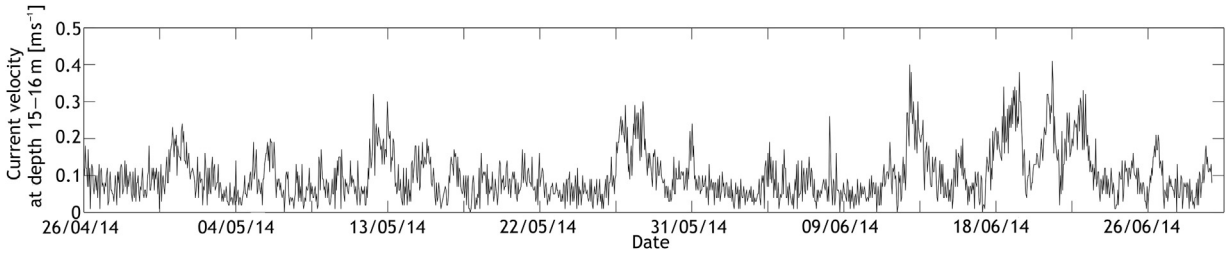

Figure 8 Time series of the mean hourly flow velocity in the nearbed layer (1–2 m above the bottom) for the time period from April 26, 2014 to June 30, 2014.

speed from Fig. 5 was used as an input in a theoretical model of wind-induced currents. The wave-induced current model is described below.

6. Methods of investigation

The investigations were focused on determining whether the motion of sediments beyond the surf zone is possible under storm conditions and how intensive it may be. In order to verify the possibility of sediment motion in the region where waves and currents had been measured, namely at a depth of 17 m, bed shear stresses were calculated for the following cases:

a) wave-induced nearbed oscillatory flow with the overall bottom roughness (the so-called "equivalent" moveable bed roughness, as defined by Kaczmarek, 1995, 1999);
b) nearbed stationary flow caused by the wind-driven current, with the bottom roughness of sand grains (the so-called "skin" bed roughness, as defined by Nielsen, 2009) and the roughness resulting from the presence of bed forms of various heights;
c) nearbed flow caused by the wind-driven current superimposed on wave-induced nearbed oscillations, with the overall bottom roughness ("equivalent" moveable bed roughness).

Sediment transport intensity is conventionally estimated using the Shields parameter, which represents the dimensionless bed shear stress and is given by the following formula (see e.g. Nielsen, 2009):

$$\theta = \frac{u_f^2}{(s-1)gd}, \tag{2}$$

in which u_f is the friction velocity, s is the ratio of sediment density ρ_s to water density ρ ($s = \rho_s/\rho$; for quartz sand: about 2.65), g denotes acceleration due to gravity, and d stands for the seabed grain diameter.

6.1. Friction velocity

A reliable and precise determination of the friction velocity u_f is difficult, particularly for unsteady currents, e.g. wave-induced nearbed oscillatory flows. The friction velocity represents the bed shear stress τ (defined as $\tau = \rho u_f^2$), which is the main driving force for sediment transport. According to the basics of fluid mechanics, the bed shear stress τ depends on the water flow velocity and the sea bottom roughness. The seabed, if built of sandy sediments, becomes moveable under hydrodynamic impacts (resulting from turbulent water flow generated by waves and currents), which causes additional difficulties in a theoretical solution leading to the determination of the friction velocity u_f. In the present study, various theoretical approaches are applied to particular cases.

The dimensionless shear stress depends on the grain diameter d. Sediment sampling and analyses show that the sand occurring at the study site (water depth h = 17 m) is very fine. The present analysis was carried out for sand grain diameter d_{50} = 0.00013 m (based on sediment grain size analysis conducted at IBW PAN).

6.2. Wind-driven current

The shear stresses τ in the water column where the wind-driven current occurs are assumed to satisfy the Boussinesq hypothesis as follows:

$$\tau = \rho \nu_t \frac{du(z)}{dz}, \tag{3}$$

where ν_t is the kinematic turbulent viscosity in the vertical direction z, and $u(z)$ is the velocity of stationary water flow.

It is further assumed that the turbulent viscosity increases linearly from the bottom, being proportional to von Karman's constant κ and the friction velocity u_f, so that

$$\nu_t = \kappa u_f z. \tag{4}$$

Bearing in mind that the shear stress can be defined as $\tau = \rho u_f^2$, one obtains the logarithmic vertical distribution of velocity $u(z)$:

$$u(z) = \frac{u_f}{\kappa} \ln\left(\frac{z}{z_0}\right), \tag{5}$$

in which z_0 denotes the ordinate at which the velocity u equals zero.

The quantity z_0 can be regarded as a theoretical seabed level from which the logarithmic profile of the velocity $u(z)$ starts. Conventionally, this level is determined as $z_0 = k_N/30$, where k_N is the so-called Nikuradse roughness. The assumption of the bottom characterised by a "skin" roughness height of $2.5d$ (due to the presence of sand grains only) yields $z_0 = 2.5d/30$. If the sea bottom is covered by bed forms, the bottom roughness height will be $z_0 = k_f/30$, where k_f is the bed form height.

The wind-driven current speed in the surface layer equals 2–5% of the wind speed w at the 10 m height above the sea level (see e.g. Kim et al., 2010). In this study, the authors consider extreme cases of measured nearbed steady flows. The analysis of the wind data and surface current velocity measurements showed that for a wind speed averaged over 12 h exceeding 7 m s^{-1} the magnitude of the surface current (in a 1 m thick layer) is about 4% of the wind speed. Thus, the following formula is assumed:

$$u_{surface} = 0.04w. \tag{6}$$

The velocity calculated by Eq. (6) is assumed to satisfy the logarithmic distribution given by Eq. (5). With the assumed bed roughness and with the resulting value of z_0, one can easily determine the friction velocity u_f from Eq. (5) if only the flow velocity u at any level z is known. The wind-driven flow velocity in the surface layer (from the mean water level to 1 m depth, namely for z = 16.5 m) is calculated by Eq. (6).

If the mean flow velocity u_{mean} is available (averaged over the water column), it is necessary to take advantage of the logarithmic velocity distribution integrated over the water depth h, from the theoretical bed level z_0 to the water surface level. After integration of the logarithmic distribution of $u(z)$ given by Eq. (5), division by the water depth h and rearrangement, the following formula for the friction velocity u_f is obtained:

$$u_f = \frac{\kappa u_{mean}}{\ln\left(\frac{h}{z_0}\right) - 1 + \frac{z_0}{h}}. \tag{7}$$

It is visible from the form of Eqs. (3)–(5) that both the friction velocity u_f and the shear stress τ are constant in the entire water column (independent of the ordinate z).

6.3. "Equivalent" moveable bed roughness

In the case of shear stresses triggered over an arbitrarily shaped sea bottom by wave-induced oscillatory nearbed flows, the approach proposed by Kaczmarek (1995) was used. The iterative procedure elaborated by Kaczmarek (1995) ensured the determination of the "equivalent" moveable bed roughness height k_e. This parameter comprises the overall roughness represented by the sand grains building the bottom and the effects of bedload. Further development of this concept by Kaczmarek (1999) led to the formulation of approximate equations describing the roughness height k_e as functions of the Shields parameter. The time-variable friction velocity $u_f(t)$ was determined by Fredsøe's integral momentum method (1984). This approach was adopted in the present study.

6.4. Waves and wind-driven current

Developed by Kaczmarek and Ostrowski (2002), the model of intensive near-bed sand transport under wave-current flow provided reliable values of sediment transport rates, successfully verified against laboratory and field data. In this model, as mentioned previously, the shear stress induced over the sea bottom characterised by the "equivalent" roughness of the moveable bed was the driving force of sediment movement. This approach was later applied by Ostrowski (2003) in the modelling of wave transformation, wave-driven currents, net sand transport and short-term morphodynamics of a multi-bar coastal zone.

For purposes of the present research, the abovementioned modelling framework was adapted to the case of the open sea (beyond the surf zone), where wave propagation under storm conditions is accompanied by the influence of a strong wind-driven current. To include this effect, the dispersion relationship for wave motion interacting with a steady flow, represented by the mean wind-driven current velocity u_{mean}, is used:

$$gk \tanh kh = (\omega - k u_{mean} \cos\alpha)^2, \tag{10}$$

where ω denotes angular frequency in the wave motion, $k = 2\pi/L$ is the wave number (L stands for the wave length), and α denotes the angle between the steady flow velocity u_{mean} and the wave propagation direction.

Similarly as in the case of wave-induced bed shear stresses, the time-variable friction velocity u_f for the bed shear stresses generated jointly by waves and the wind-driven current is determined using the theoretical concept of Kaczmarek and Ostrowski (2002).

The analysis of current data available for the period from April 26, 2014 to June 30, 2014 revealed extreme flow conditions (with the maximum measured velocity in the nearbed water layer) on June 12, 2014 and June 21, 2014.

As deduced by Kaczmarek and Ostrowski (1995, 1996), bed shear stresses and sediment transport rates under natural conditions (for irregular waves actually observed at sea) can be reliably modelled by the linear wave theory, using the root-mean-square wave height (H_{rms}) and the peak wave energy period (T_p) as inputs. Therefore, the bed shear stresses generated by waves and wave–current interactions were computed using the wave parameters H_{rms} and T_p. The values of H_{rms} and T_p corresponding to the extreme nearbed current velocities were obtained from the analysis of the wave data collected in the region considered (with water depth h = 17 m). The wave parameters constituted a basis for the determination of wave-induced nearbed oscillatory

currents. All these quantities, together with other parameters (h, d_{50} and w), were used in the theoretical modelling of the bed shear stresses under various hydrodynamic impacts.

The model of the wind-induced current and shear stresses generated by this current was verified by current profiles measured on June 12, 2014 and June 21, 2014 at the location considered.

7. Current data

The results of statistical analysis of measurement data are presented in Tables 1–4.

As could be expected, the lowest flow velocities, both time-averaged and maximal, were recorded in the nearbed layer, and the highest velocities occurred close to the water surface (Table 1). It can be seen in Table 2 that magnitudes exceeding 0.2 m s^{-1} occurred in the nearbed layer (1–2 m above the bottom) for 19.5% of time (12.5 days). Table 3 shows that the dominant directions of flow within the whole water column were in the eastern sector (*flow towards*), which coincides with the dominant direction of the wind. The second most dominant directions of flow were in the western sector. Table 4 indicates that the most common velocity in this layer was between 0.1 and 0.15 m s^{-1}. Table 4 also shows that a relatively frequent velocity within all layers ranged from 0.05 to 0.2 m s^{-1} and that the flow exceeding 0.2 m s^{-1} lasted on average for 30% of the time.

8. Results and discussion

As already mentioned, two cases corresponding to extreme conditions during measurements were used to compare the measured steady current velocity profile with the modelled one using Eqs. (5) and (6), as well as to determine bed shear stresses for various hydrodynamic impacts. The input parameters are given in Table 5.

Table 1 Statistical data from flow measurements for the time period from April 26, 2014 to June 30, 2014.

Distance from bottom (z) [m]	Period April 26, 2014–June 30, 2014	
	Mean velocity [m s^{-1}]	Maximum velocity [m s^{-1}]
16–17	0.29	0.75
15–16	0.15	0.58
14–15	0.13	0.58
13–14	0.13	0.56
12–13	0.13	0.57
11–12	0.12	0.53
10–11	0.12	0.51
9–10	0.12	0.5
8–9	0.12	0.47
7–8	0.12	0.46
6–7	0.11	0.45
5–6	0.11	0.48
4–5	0.11	0.47
3–4	0.11	0.45
2–3	0.10	0.41
1–2	0.10	0.41

Table 2 Frequency of occurrence of individual velocities in the nearbed layer (1–2 m from the bottom) for the time period from April 26, 2014 to June 30, 2014.

Velocity values [m s^{-1}]	Frequency [%]	Length of occurrence [days]
>0.3	3.9	2.5 (60 h)
<0.2; 0.3)	15.6	10 (240 h)
<0.1; 0.2)	60.7	38.8 (932 h)
<0.05; 0.1)	19.3	12.4 (297 h)
<0.05	0.5	0.29 (7 h)

Table 3 Flow direction frequency of occurrence in all measured layers for 12-h averaged wind velocities exceeding 7 m s^{-1} for the time period from April 26, 2014 to June 30, 2014.

Frequency [%] / Direction	Distance from bottom [m]																
	Wind	16–17	15–16	15–14	14–13	13–12	12–11	11–10	10–9	9–8	8–7	7–6	6–5	5–4	4–3	3–2	2–1
N	2.5	1.4	3.3	4.3	1.8	2.9	2.3	2.5	2.1	1.9	1.9	2.1	1.4	2.7	1.9	1.9	1.4
NNE	0.0	0.8	0.2	1.0	1.0	0.8	1.4	1.0	0.0	0.4	1.2	1.0	0.6	1.0	1.2	2.1	1.0
NEE	5.1	1.4	1.2	2.3	2.1	2.1	2.9	2.9	3.3	3.7	3.9	2.3	4.5	3.7	5.4	6.8	5.1
E	19.1	16.9	15.0	19.8	20.6	24.1	21.0	20.4	24.9	23.9	25.1	24.9	23.5	24.7	22.0	22.8	25.5
SEE	18.1	23.7	29.2	22.0	22.8	19.3	21.6	24.3	20.4	23.1	20.2	20.4	21.4	20.6	18.5	15.8	15.8
SSE	2.9	6.8	3.5	4.3	3.7	2.9	3.5	2.3	1.2	1.4	2.1	3.9	2.9	2.1	3.3	2.9	2.1
S	6.6	0.8	1.9	2.3	1.7	2.9	1.9	0.8	1.0	1.2	1.4	1.2	1.4	1.9	2.5	2.7	2.3
SSW	5.6	1.7	1.9	1.0	1.4	1.8	1.2	1.8	2.5	2.1	2.5	2.1	2.3	1.4	4.5	4.3	7.6
SWW	19.1	4.3	5.8	2.3	2.5	4.3	3.5	3.1	3.9	5.1	4.5	4.3	6.6	7.8	8.0	9.3	12.8
W	6.6	14.0	14.8	9.9	8.6	8.8	12.1	13.8	14.8	15.2	18.5	19.3	21.4	19.7	20.8	22.0	18.3
NWW	3.5	15.0	18.5	25.5	27.8	24.5	25.3	23.4	21.4	18.7	14.8	16.0	10.7	10.9	8.8	7.8	6.0
NNW	10.9	13.2	4.7	5.3	6.0	5.6	3.3	3.7	4.5	3.3	3.9	2.5	3.3	3.5	3.1	1.6	2.1

Legend	[%]	0–1	2–3	4–5	6–7	8–9	10–11	12–13	14–15	16–17	18–19	20–21	22–23	24–25	26–27	28–29
	Color															

Table 4 Flow velocity frequency of occurrence in all measured layers for the time period from April 26, 2014 to June 30, 2014.

Frequency [%] / Velocity [m s^{-1}]	Distance from bottom [m]															
	16–17	15–16	15–14	14–13	13–12	12–11	11–10	10–9	9–8	8–7	7–6	6–5	5–4	4–3	3–2	2–1
0–0.05	0.0	0.2	0.1	0.2	0.3	0.1	0.2	0.3	0.5	0.5	0.4	0.4	0.4	0.1	0.3	0.5
0.05–0.1	3.9	13.6	17.6	17.7	19.5	21.2	22.1	23.3	22.5	22.9	22.9	24.0	24.6	25.5	25.5	27.9
0.1–0.15	9.2	23.8	28.1	28.0	28.7	29.8	28.6	28.1	28.1	30.3	31.8	31.0	31.5	33.4	36.1	35.6
0.15–0.2	7.7	22.00	21.9	24.2	22.3	19.2	21.9	21.2	23.0	19.4	21.7	19.7	20.8	20.1	19.1	19.3
0.2–0.25	9.0	17.2	14.8	12.2	12.2	14.1	11.4	11.4	10.8	11.6	10.6	12.2	10.7	10.6	10.0	9.1
0.25–0.3	9.4	9.8	6.4	7.9	7.7	7.0	7.2	7.9	7.2	8.2	6.1	7.0	6.0	6.1	4.6	4.1
0.3–0.35	13.9	7.6	6.3	5.3	5.1	4.7	4.9	3.5	4.5	3.8	3.5	3.1	3.3	2.0	2.9	2.5
0.35–0.4	14.1	3.0	2.4	2.1	2.0	1.9	1.9	2.1	1.8	2.0	1.7	1.3	1.8	1.6	1.2	0.8
0.4–0.45	9.8	1.2	0.7	1.2	0.8	0.7	0.7	1.1	0.7	0.9	1.1	0.8	0.4	0.4	0.3	0.1
0.45–0.5	10.9	0.7	0.8	0.5	0.6	0.7	0.5	0.7	0.8	0.4	0.2	0.4	0.5	0.3	0.1	0.1
>0.5	11.9	1.0	0.9	0.7	0.8	0.7	0.5	0.4	0.1	0.1	0.1	0.1	0.1	0.1	0.0	0.0

Legend [%]	0–1	2–3	4–5	6–7	8–9	10–11	12–13	14–15	16–17	18–19	20–21	22–23	24–25	26–27	28–29	30–31	32–33

Table 5 Input parameters for modelling the wind-driven current and bed shear stresses for two hydrodynamic impacts.

Parameters	Case 1	Case 2
Date	June 12, 2014	June 21, 2014
H_{rms}	0.76 m	1.41 m
T_p	5.85 s	6.42 s
w	11.16 m s^{-1}	10.22 m s^{-1}
α	10°	40°

8.1. Flow velocities

The results of flow measurements and computations are shown in Figs. 9–12.

It can be seen in Figs. 9 and 11 that agreement between the measured and modelled flow velocity profiles is reasonably good, irrespective of the assumed bottom roughness k_N.

The analysis of the field data showed that the measured mean flow velocities in the entire water column had almost the same direction as the wind. This is visible in Figs. 10 and 12.

8.2. Bed shear stresses

As already pointed out, the bed shear stress causes sediment transport, and the dimensionless shear stress θ is an indicator of the sediment motion intensity. Bed shear stresses were modelled for the hydrodynamic cases and with the input quantities described in Section 3. For the case of bed shear stresses (represented by the Shields parameter θ) induced solely by the wind-driven current, aside from the "skin" bed roughness ($k_N = 2.5d$), two values of the bed form roughness were assumed, namely $k_f = 0.05$ m and $k_f = 0.10$ m. For the cases of the wave-induced shear stress and the shear stress induced by waves and currents, the Shields parameter θ_{max} was calculated from the friction velocity $u_{fmax} = \max[(u_f(\omega t)]$. The results of modelling are given in Tables 6–8.

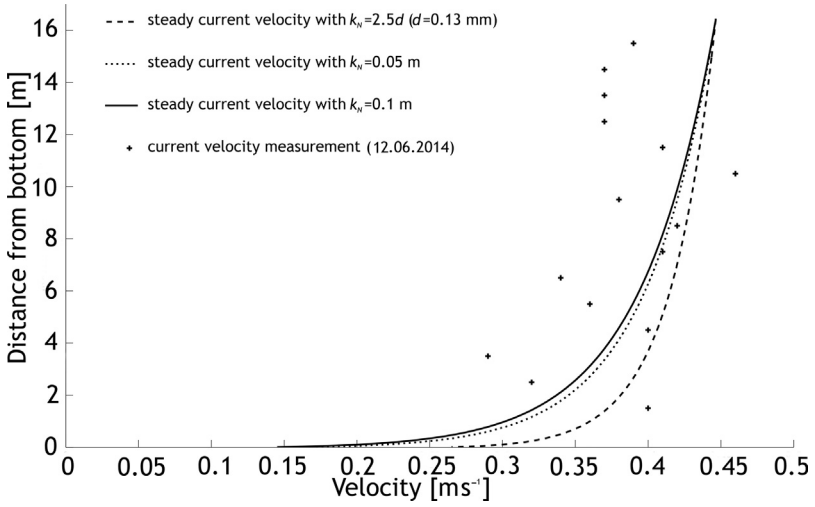

Figure 9 Velocity profiles of steady wind-driven current for different k_N and measured velocity on June 12, 2014 (case 1).

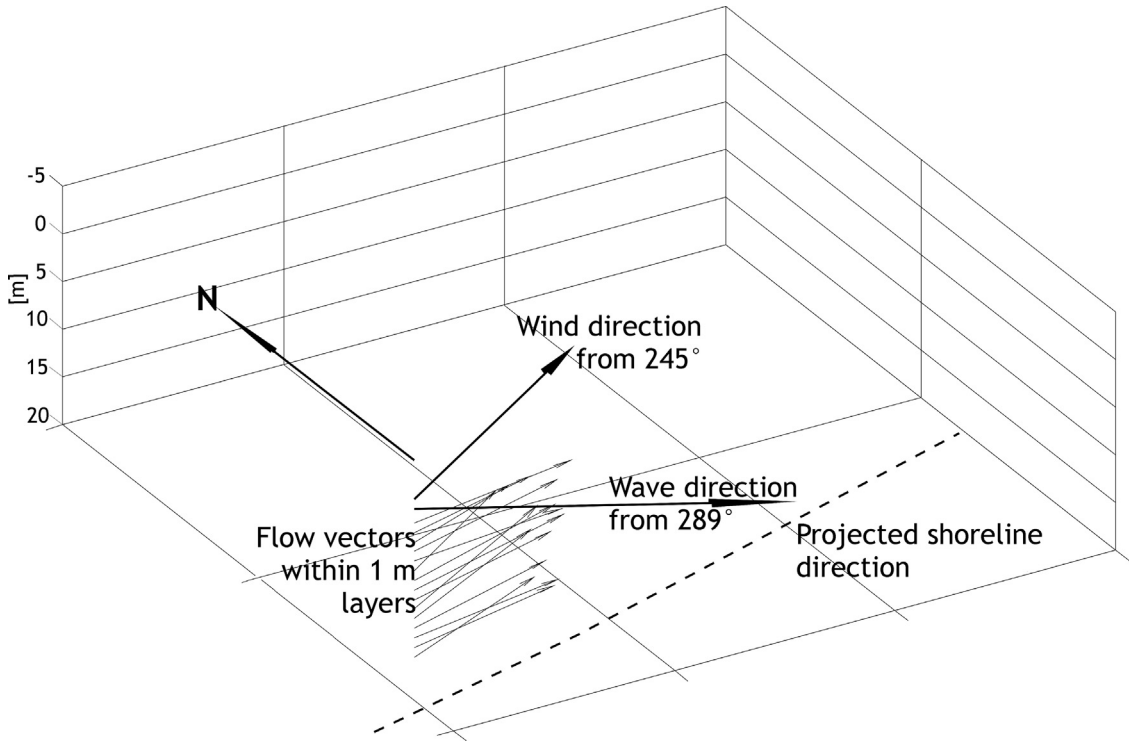

Figure 10 Scheme of measured current vectors together with wind and peak wave direction on June 12, 2014 (case 1).

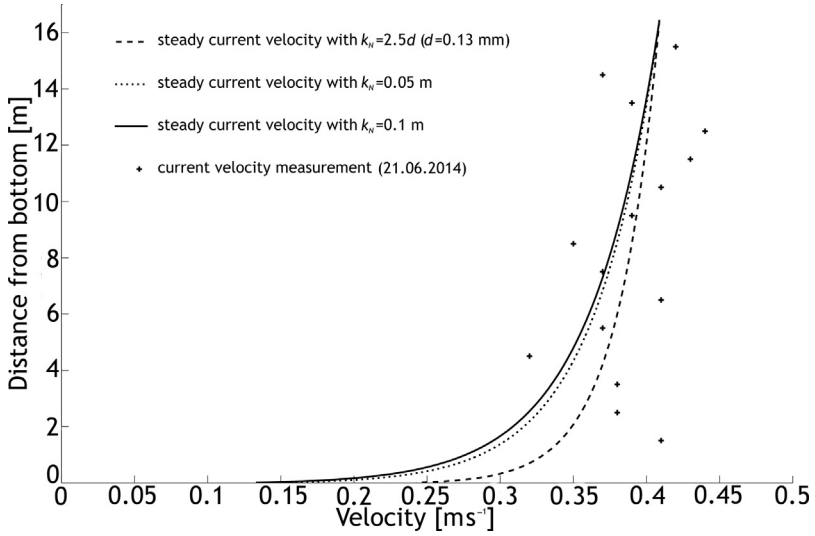

Figure 11 Velocity profiles of steady wind-driven current for different k_N and measured velocity on June 21, 2014 (case 2).

The quantity U_{1m} in Table 6 is the maximum nearbed wave-induced (free stream) oscillatory velocity (for sinusoidal waves, $U(\omega t) = U_{1m} \sin(\omega t)$).

In analysing the results of θ computations, the following regimes of sediment transport were assumed:

$\theta \in <0; 0.05>$ no sediment motion;
$\theta \in (0.05; 0.3>$ very weak sediment motion; ripples appear on the seabed;
$\theta \in (0.3; 0.6>$ weak sediment motion; ripples develop;
$\theta \in (0.6; 0.9>$ moderately intensive sediment motion; ripple height decreases;
$\theta > 0.9$ intensive sediment motion (sheet flow), flat seabed.

The results of calculations shown in Table 6 (dimensionless maximum wave-induced bed shear stress θ_{max} with the "equivalent" bottom roughness) indicate that, under the wave conditions considered, seabed grains with a diameter of 0.13 mm move very little (case 1) or little (case 2). The corresponding values of θ_{max} amounting to 0.227 and

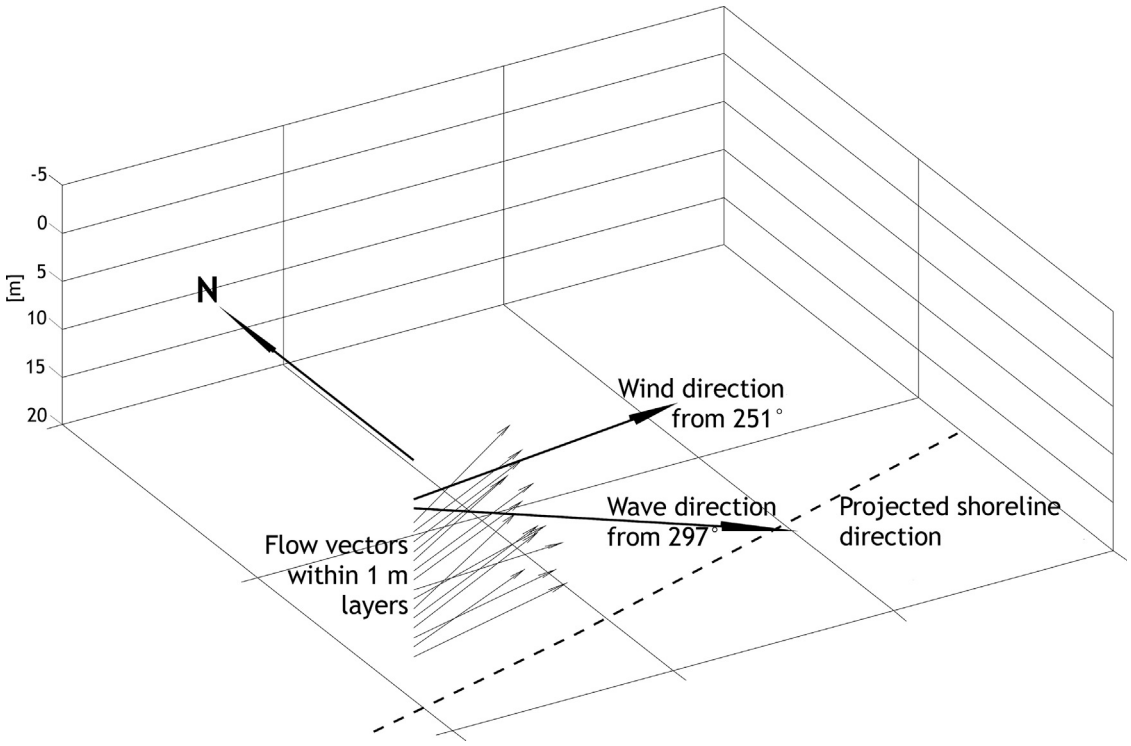

Figure 12 Scheme of measured current vectors together with wind and peak wave direction on June 21, 2014 (case 2).

Table 6 Wave-induced bed shear stress with "equivalent" bottom roughness.

	Case 1	Case 2
U_{1m}	0.105	0.245
u_{fmax}	0.008	0.033
θ_{max}	0.227	0.514

Table 7 Bed shear stress induced by wind-driven current.

	$k_N = 2.5d$	$k_N = k_f = 0.05$ m	$k_N = k_f = 0.1$ m
Case 1			
u_{mean}	0.420	0.399	0.395
u_f	0.013	0.019	0.021
θ	0.069	0.191	0.224
Case 2			
u_{mean}	0.380	0.365	0.361
u_f	0.012	0.018	0.019
θ	0.067	0.161	0.188

0.514 indicate development of ripple marks. Dimensionless bed shear stresses θ determined for the case of the sole wind-driven current under the conditions considered (Table 7), in comparison with wave-induced hydrodynamics and the "equivalent" bed roughness (Table 6), are distinctly smaller for all assumed bed roughness values, lying in the range from 0.067 to 0.224, which corresponds to very slight motion of grains.

The most interesting case is that of the nearbed wave–current interaction. Shown in Table 8, the results of the modelling of the dimensionless bed shear stresses θ_{max} generated jointly by waves and the wind-driven current indicate that the sandy material under the conditions and at the site considered is subject to rather intense movement. Further, it appears that the values of θ_{max} given in Table 8 are higher than the sums of their counterparts (θ_{max} and θ) given in Tables 6 and 7. This nonlinear effect clearly implies a synergic character of wave–current interaction as a prime mover of marine lithodynamics.

Table 8 Bed shear stress induced by nearbed wave–current interaction.

	$k_N = 2.5d$	$k_N = k_f = 0.05$ m	$k_N = k_f = 0.1$ m
Case 1			
u_{fmax}	0.035	0.034	0.033
θ_{max}	0.567	0.537	0.532
Case 2			
u_{fmax}	0.0401	0.0397	0.0397
θ_{max}	0.764	0.748	0.748

It is worth noting that the values of u_{fmax} and θ_{max} shown in Table 8 are little dependent on the bed roughness k_N. This is typical of the wave-dominated bed boundary layer, which is weakly affected by the steady current. On the other hand, the steady current can be affected by the wave-dominated bed boundary layer constituting a larger apparent bottom roughness (see discussion by Ostrowski and Stella, 2016).

The values of bed shear stresses obtained for severe storm conditions occurring in the period considered are relatively high, exceeding the critical quantities for the motion of sand grains. Such results can explain sediment motion and the silting up of bottom excavations at significant depths, as well

as the appearance and migration of bed forms in a non-tidal sea (the south Baltic), observed by Rudowski et al. (2008) and Uścinowicz et al. (2014).

9. Final remarks and conclusions

According to Nielsen (2009), rapidly accelerated flows induced by waves have thinner bed boundary layers than longer period flows (such as tidal currents). Consequently, wave motions generate greater bed shear stresses for a given free stream velocity magnitude. This rule is confirmed by the results of the present study. The bed shear stresses determined for the wave-induced oscillatory flow are bigger than the ones determined for the wind-driven steady current although the wave-induced nearbed maximum velocity U_{1m} is smaller than the steady current velocity averaged over the water column (u_{mean}).

It was found that, for the cases considered, the measured mean flow velocities in the entire water column had almost the same direction as the wind. Hence, it appears that at the limited depths of the Baltic Sea the wind-driven current velocity profile can be described by a directionally invariable distribution.

For the site considered, the modelling of bed shear stresses for various extreme hydrodynamic impacts yields the highest values of the Shields parameter θ in the case of a joint action of waves and the wind-driven current. It appears that nonlinear wave–current interaction generates bed shear stresses bigger than would result from the superposition of results determined separately for the impacts of waves and currents. The calculated bed shear stresses are high enough to generate sediment transport.

The relatively intensive hydrodynamic conditions at a depth of 17 m, however, have an instantaneous character in the scale of a year. The question arises whether these conditions, given their relatively short duration, can explain the appearance and migration of bed forms, especially large forms, such as sand waves. It can be supposed that the significant seabed changes observed (Rudowski et al., 2008) result from extreme wave-current conditions occurring repeatedly in longer time scales, e.g. over a few years. Clarification of the above doubts requires a more detailed quantitative insight into sediment transport present beyond the surf zone. In particular, measurements of nearbed velocities combined with observations of seabed evolution at a depth of 15–25 m would shed new light on the hydrodynamic and lithodynamic processes taking place in this region.

Acknowledgements

The study was sponsored by the Ministry of Science and Higher Education, Poland, under mission-related programme No. 2 of IBW PAN and by the National Science Centre, Poland, under project No. PBS1/A6/8/2012.

References

Belibassakis, K.A., Karathanasi, F.E., 2017. Modelling nearshore hydrodynamics and circulation under the impact of high waves at the coast of Varkiza in Saronic-Athens Gulf. Oceanologia 59 (3), 350–364, http://dx.doi.org/10.1016/j.oceano.2017.04.001.

Birkemeier, W.A., 1985. Field data on seaward limit of profile change. J. Waterway Port Coast. Ocean Eng. 111 (3), 598–602, http://dx.doi.org/10.1061/(ASCE)0733-950X(1985)111:3(598).

Carbajal, N., Montaño, Y., 2001. Comparison between predicted and observed physical features of sandbanks. Estuar. Coast. Shelf Sci. 52 (14), 435–443, http://dx.doi.org/10.1006/ecss.2000.0760.

Cerkowniak, G.R., Ostrowski, R., Stella, M., 2015a. Depth of closure in the multi-bar non-tidal nearshore zone of the Baltic Sea: Lubiatowo (Poland) case study. Bull. Maritime Inst. Gdańsk. 30 (1), 180–188, http://dx.doi.org/10.5604/12307424.1185577.

Cerkowniak, G.R., Ostrowski, R., Stella, M., 2015b. Wave-induced sediment motion beyond the surf zone: case study of Lubiatowo (Poland). Arch. Hydro-Eng. Environ. Mech. 62 (1–2), 27–39, http://dx.doi.org/10.1515/heem-2015-0017.

Cerkowniak, G.R., Ostrowski, R., Pruszak, Z., 2017. Application of Dean's curve to investigation of a long-term evolution of the southern Baltic multi-bar shore profile. Oceanologia 59 (1), 18–27, http://dx.doi.org/10.1016/j.oceano.2016.06.001.

Dean, R.G., 2002. Beach Nourishment. Theory and Practice. Advanced Series on Ocean Engineering, vol. 18. World Sci. Publ. Co. Pte. Ltd., 399 pp.

Fredsøe, J., 1984. Turbulent boundary layer in combined wave-current motion. J. Hydraul. Eng. 110 (8), 1103–1120, http://dx.doi.org/10.1061/(ASCE)0733-9429(1984)110:8(1103).

Hallermeier, R.J., 1978. Uses for a calculated limit depth to beach erosion. In: Proceedings, 16th Coastal Engineering Conference. American Society of Civil Engineers, 1493–1512.

Hallermeier, R.J., 1981. A profile zonation for seasonal sand beaches from wave climate. Coast. Eng. 4 (3), 253–277.

Hulscher, S.J.M.H., van den Brink, G.M., 2001. Comparison between predicted and observed sand waves and sand banks in the North Sea. J. Geophys. Res. 106 (C5), 9327–9338, http://dx.doi.org/10.1029/2001JC900003.

Kaczmarek, L.M., 1995. Nonlinear effects of waves and currents on moveable bed roughness and friction. Arch. Hydro-Eng. Environ. Mech. 42 (1–2), 3–27.

Kaczmarek, L.M., 1999. Moveable Sea Bed Boundary Layer and Mechanics of Sediment Transport. (D.Sc. thesis). IBW PAN, Gdańsk, 209 pp.

Kaczmarek, L.M., Ostrowski, R., 1995. Modelling of bed shear stress under irregular waves. Arch. Hydro-Eng. Environ. Mech. 42 (1–2), 29–51.

Kaczmarek, L.M., Ostrowski, R., 1996. Bedload under asymmetric and irregular waves: theory versus laboratory data. Arch. Hydro-Eng. Environ. Mech. 43 (1–4), 21–42.

Kaczmarek, L.M., Ostrowski, R., 2002. Modelling intensive near-bed sand transport under wave-current flow versus laboratory and field data. Coast. Eng. 45 (1), 1–18, http://dx.doi.org/10.1016/S0378-3839(01)00041-2.

Kim, S.Y., Cornuelle, B.D., Terrill, E.J., 2010. Decomposing observations of high-frequency radar derived surface currents by their forcing mechanisms: locally wind-driven surface currents. J. Geophys. Res. 115 (C12), http://dx.doi.org/10.1029/2010JC006223.

Krauss, W., 2001. Chapter: Baltic sea circulation. In: Steele, J., Thorpe, S., Turekian, K. (Eds.), Encyclopedia of Ocean Sciences. Acad. Press, 236–244, http://dx.doi.org/10.1006/rwos.2001.0381.

Nielsen, P., 2009. Coastal and Estuarine Processes. Advanced Series on Ocean Engineering, vol. 29. World Sci. Publ. Co. Pte. Ltd., 343 pp.

Ostrowski, R., 2003. A quasi phase-resolving model of net sand transport and short-term cross-shore profile evolution. Oceanologia 45 (2), 261–282.

Ostrowski, R., Schönhofer, J., Szmytkiewicz, P., 2015. South Baltic representative coastal field surveys, including monitoring at the Coastal Research Station in Lubiatowo, Poland. J. Mar. Syst. 162, 89–97, http://dx.doi.org/10.1016/j.jmarsys.2015.10.006.

Ostrowski, R., Stella, M., 2016. Sediment transport beyond the surf zone under waves and currents of the non-tidal sea: Lubiatowo (Poland) case study. Arch. Hydro-Eng. Environ. Mech. 63 (1), 63—77.

Pruszak, Z., Szmytkiewicz, P., Ostrowski, R., Skaja, M., Szmytkiewicz, M., 2008. Shallow-water wave energy dissipation in a multi-bar coastal zone. Oceanologia 50 (1), 43—58.

Rudowski, S., Łęczyński, L., Gajewski, Ł., 2008. Sand waves on the bottom of the deep nearshore and their role in shore formation. Landf. Anal. 9, 214—216, (in Polish).

Sokolov, A., Chubarenko, B., 2012. Wind influence on the formation of nearshore currents in the southern Baltic: numerical modelling results. Arch. Hydro-Eng. Environ. Mech. 59 (1—2), 37—48.

Trzeciak, S., 2000. Marine Meteorology with Oceanography. PWN, 249 pp., (in Polish).

Uścinowicz, S., Jegliński, W., Miotk-Szpiganowicz, G., Nowak, J., Pączek, U., Przezdziecki, P., Szefler, K., Poręba, G., 2014. Impact of sand extraction from the bottom of the southern Baltic Sea on the relief and sediments of the seabed. Oceanologia 56 (4), 857—880, http://dx.doi.org/10.5697/oc.56-4.857.

Valle-Levinson, A., 2016. Lecture 13. Equations of Motion, web location: http://www.essie.ufl.edu/ ~arnoldo/ocp6050/notes_pdf/ (31.05.16).